Journal of Materials Science & Technology 68 (2021) 70–75

Contents lists available at ScienceDirect

Journal of Materials Science & Technology

journal homepage: www.jmst.org

Research Article

High-throughput simulation combined machine learning search for optimum elemental composition in medium entropy alloy

Jia Li [a], Baobin Xie [a], Qihong Fang [a,*], Bin Liu [b], Yong Liu [b], Peter K. Liaw [c]

[a] State Key Laboratory of Advanced Design and Manufacturing for Vehicle Body, Hunan University, Changsha, 410082, China
[b] State Key Laboratory of Powder Metallurgy, Central South University, Changsha, 410083, China
[c] Department of Materials Science and Engineering, The University of Tennessee, Knoxville, TN, 37996, USA

ARTICLE INFO

Article history:
Received 16 April 2020
Received in revised form 22 May 2020
Accepted 4 June 2020
Available online 9 August 2020

Keywords:
Medium entropy alloy
Optimum elemental composition
High-throughput simulation
Machine learning

ABSTRACT

In medium/high entropy alloys, their mechanical properties are strongly dependent on the chemical-elemental composition. Thus, searching for optimum elemental composition remains a critical issue to maximize the mechanical performance. However, this issue solved by traditional optimization process via "trial and error" or experiences of domain experts is extremely difficult. Here we propose an approach based on high-throughput simulation combined machine learning to obtain medium entropy alloys with high strength and low cost. This method not only obtains a large amount of data quickly and accurately, but also helps us to determine the relationship between the composition and mechanical properties. The results reveal a vital importance of high-throughput simulation combined machine learning to find best mechanical properties in a wide range of elemental compositions for development of alloys with expected performance.

1. Introduction

Making lighter, stronger, and cheaper materials is an extremely-important area in alloys, which determines their widespread structural applications. The recent developed multi-principal element alloys such as medium entropy alloys (MEAs) and high-entropy alloys (HEAs) have been studied extensively in terms of their corrosion resistance, irradiation resistance, tensile (compression) behaviour, fracture toughness and creep resistance [1–10]. They attract high attention as they offer a largely unexplored elemental compositions, making an opportunity for detecting novel properties. Yet, for designing HEAs with enhanced mechanical properties and more economical development, building relationship between elemental composition and properties is essential [11–15].

With the advancement of computer capabilities, theoretical modeling, and simulation methods, it can be possible to use high-throughput simulations to quickly search, discover, or optimize the performance of materials. Before the actual experiment, we can use high-throughput simulation to quickly search a large number of existing or non-existent, all possible compounds according to the specific performance optimization. Meanwhile, high-throughput first-principles or molecular dynamics (MD) simulations help us to establish the relationship between structures and properties on a microscopic and mesoscopic scale. It can provide sufficient data information for the design of new materials, eliminating "trial-and-error" process [16–18]. Recently, high-throughput simulation methods have been successfully applied to the design and discovery of secondary lithium battery materials [19,20]. Based on high-throughput first-principles, the properties of thousands of secondary lithium battery materials can be calculated, thereby screening out the reasonable materials with desired properties [19,20]. In this work, we use high-throughput MD simulation, to quickly establish a composition-performance database.

However, huge amounts of data obtained by high-throughput simulation has the characteristics of high dimensional input-low dimensional output, which is difficult to be described by traditional mathematical modeling. Machine learning is a state-of-the-art computer technology, which can be used to identify the correlations between data. Machine learning can learn from the training dataset independently, and gains its own insights without the need for explicit programming [21]. Early machine learning is usually employed in image recognition and speech recognition. Recently, machine learning has been widely used in material science [22–25]. Machine learning contains many algorithms, such as genetic algorithm, random forest algorithm, support vector machine algorithm

* Corresponding author.
E-mail address: fangqh1327@hnu.edu.cn (Q. Fang).

https://doi.org/10.1016/j.jmst.2020.08.008
1005-0302/

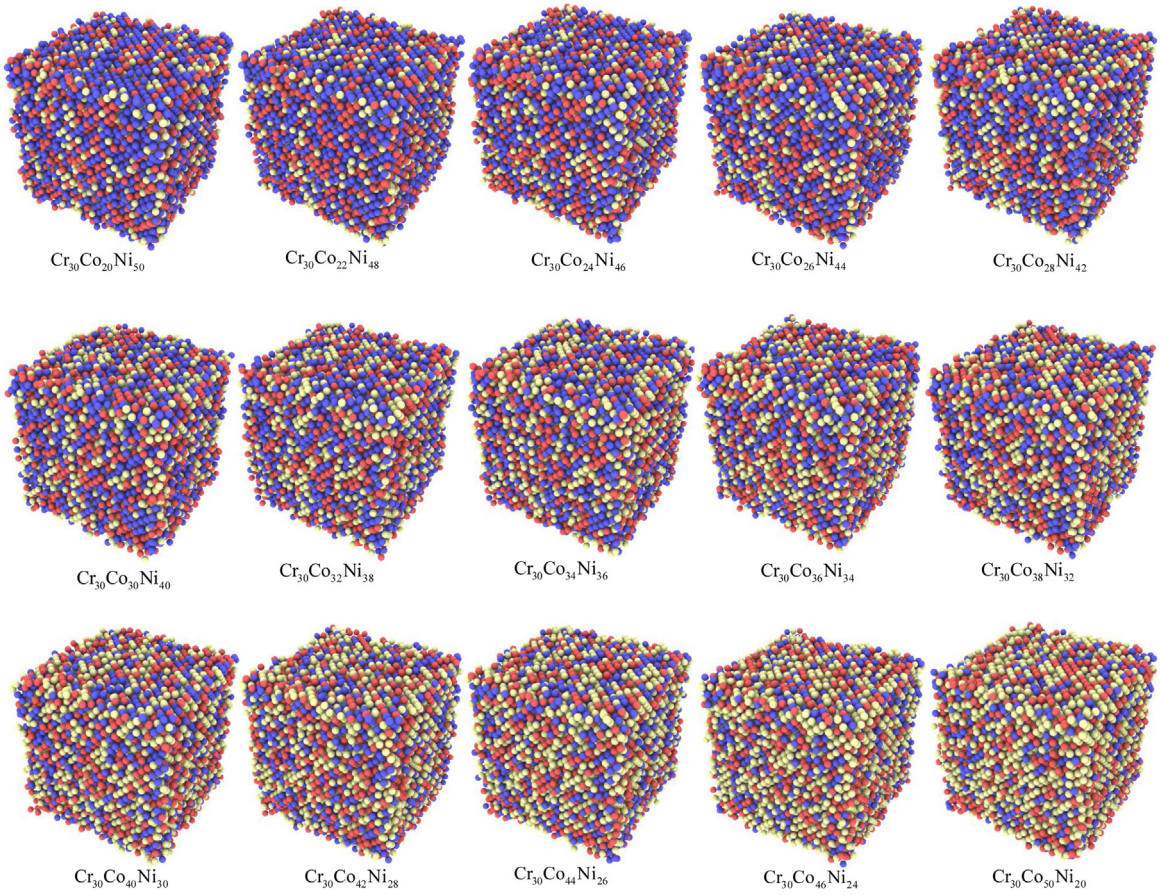

Fig. 1. The elemental distributions of $Cr_{30}Co_yNi_{70-y}$ MEA. Cr, Co, and Ni.

[26], and the artificial neural network (ANN). Especially, ANN has been widely used in development and design of new materials. For example, the back-propagation algorithm (BP) neural network combining with genetic algorithm is used to establish the inference model of the mechanical properties in low alloy steel by the composition and heat treatment conditions [27]. A multilayer ANN model is used to predict the yield strength, ultimate tensile strength, and elongation in CuSnPbZnNi alloy [28]. In general, machine learning can capture the highly-complex non-linear input/output relationships, to help filter or select the potential good alloys rapidly and accurately in material science.

In the present work, using the high-throughput MD simulation combined machine learning, we can predict the optimum elemental composition for $Cr_xCo_yNi_{100-x-y}$ MEA with high strength and low cost/density. Our results indicate the possibility to find the best mechanical properties in a wide range of elemental compositions based on high-throughput MD simulation data. Comparing with the traditional "trial and error" method or experiences of domain experts, "high-throughput MD simulation combined machine learning" method not only obtains a large amount of data quickly and accurately, but also helps us to establish the accurate relationship between the composition and performance in $Cr_xCo_yNi_{100-x-y}$ MEA. Importantly, the composition range obtained in MEAs with the best mechanical properties can provide the initial reference value to guide the experiment accurately. The work has the potential to boost the speed of the MEA research fundamentally and provide implications for the design of advanced materials with target properties. In addition, a new approach "High-throughput MD simulation combined machine learning" is proposed to tackle the challenge of established composition-property relationship.

2. Methods

2.1. MD simulation

The deformation behavior of $Cr_xCo_yNi_{100-x-y}$ MEA ($20 \leq x \leq 60$ at.%, and $20 \leq y \leq 60$ at.%) is presented using MD simulations, as shown in Fig. 1. Thus, the element concentrations of Cr, Co, and Ni range from 20 % to 60 %, to meet the conditions of the CrCoNi MEA in which every element concentration is higher than 20 % and less than 60 %. The bulk MEA samples with dimensions of 53 Å (x) $\times$53 Å (y) $\times$53 Å (z) contain 13,500 atoms. The orientation of the MEA sample is [100] along the x direction, [010] along the y direction, and [001] along the z direction. The modified embedded atom method (MEAM) potentials are used to study the yielding strength of the $Cr_xCo_yNi_{100-x-y}$ MEA [29]. The time step of the MD simulation is 1 fs. During the simulation, the initial configuration is built by randomly substituting an FCC lattice with different elements, and every type atom is randomly placed. The temperature of samples is 300 K, and then MEAs are stretched along the x axis under a constant strain rate of 1×10^8 s^{-1} at a temperature of 300 K. Periodic boundary conditions (PBCs) are imposed in all directions.

2.2. Machine learning

To search for the optimal elemental concentration in the $Cr_xCo_yNi_{100-x-y}$ MEA, a machine-learning-based approach coupled with the high-throughput MD simulation is used to predict the relationship between elemental concentrations and ultimate tensile strengths. Our machine-learning design system consists of five major processes in Fig. 2, including building of the data sets, train-

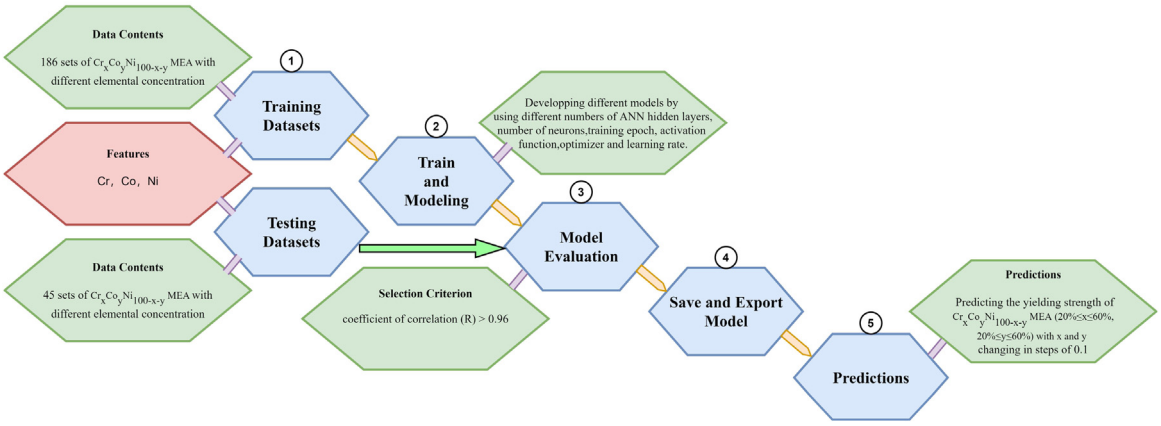

Fig. 2. Flow chart of the machine-learning design system for rapid and accurate compositional design.

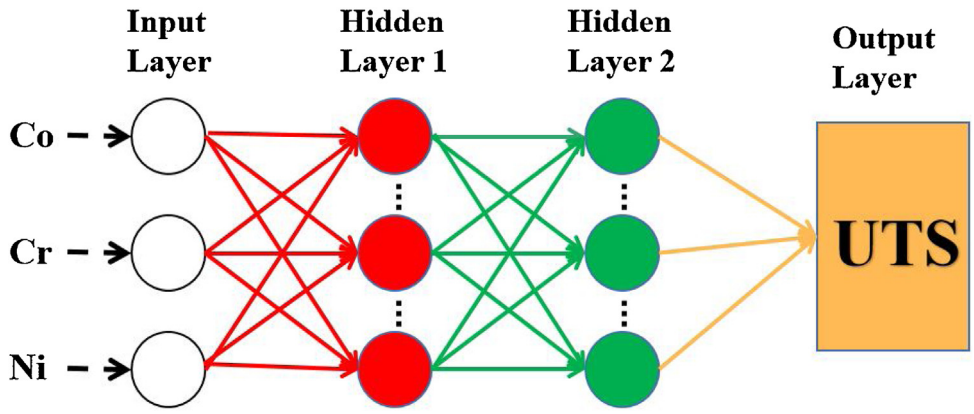

Fig. 3. An architecture of a multi-layer feed-forward ANN consisting of an input layer, two hidden layers, and one output layer.

ing and modeling, model evaluation, save and export model, and predictions.

The details are as follows: (i) The training data sets and testing data sets include 186 and 45 sets of $Cr_xCo_yNi_{100-x-y}$ MEAs with different elemental concentrations; (ii) The machine learning model is built by keras (the python deep learning library), in which six parameters, numbers of ANN hidden layers, numbers of neurons, activation function, optimizer, training epoch and learning rates can be tuned to develop different models. Generally, increasing the number of hidden layers is to better adapt to the case of large samples, but this is at the expense of computing costs. In addition, if the number of the samples is fixed, excessive increase of the number of hidden layers can not improve the accuracy of the model [30]. At present, there is no direct functional relationship between the number of hidden layers and the number of samples, so we can only use the one-by-one test method to determine the optimal number of hidden layers. Here, the architecture with only one hidden layer can not solve the complex problem of quintuple regression, meaning that the test accuracy is very low. In addition, the architecture with three or more hidden layers would also be tested. The accuracy of the machine learning model is almost the same, but they are linked to the larger amount of calculation. We employ the Sigmoid function [31] as the activation function of the hidden layer, which can be written as $\sigma(x) = \frac{1}{1+e^{-x}}$. The Sigmoid function transforms the input variable into values between 0 and 1, which makes the values of the input variable difficult to diverge during the transfer process. Because the Sigmoid function is not sensitive to extreme values, the influence of extreme values on training results can be largely eliminated. Choosing the appropriate learning rate, optimizer and the number of neurons in each layer can not only improve the training efficiency, but also ensure that the convergence is faster and the error is minimized in the training process [32]. Through trial and error method, we use 10 as the learning rate and the number of neurons in each layer. Adamoptimizer is employed as the optimizer for model compilation, and the learning rate of the adamoptimizer is set to be 0.01. Fig. 3 illustrates the ANN architecture employed in present work. (iii) The best model is selected from the trained models by coefficient of correlation (R) > 0.96. (iv) Save and export model for prediction; (v) The best model is used to predict the ultimate tensile strength of $Cr_xCo_yNi_{100-x-y}$ MEAs with different elemental concentrations.

3. Results and discussion

Fig. 4(a–d) plots the predicted ultimate tensile strength values in the machine-learning model as a function of the simulated ultimate tensile strength values of the training set, validation set, testing set and all data, respectively. The data points fall along the dotted line, indicating that the predicted values are very consistent with the simulated values. We further linearly fit the predicted value with the simulated value, as shown by the solid line. The closer the solid line is to the dotted line, the better the performance of the machine-learning model. It can be seen that our model performs very well on the training set, validation set, testing set, and all data.

In machine learning algorithm, with the increase of training epoch, mean squared error (MSE) of training set would gradually decrease, which makes the accuracy of machine learning model higher. However, when the MSE of the training set decreases to a certain extent, increasing the training epoch leads to the MSE of the

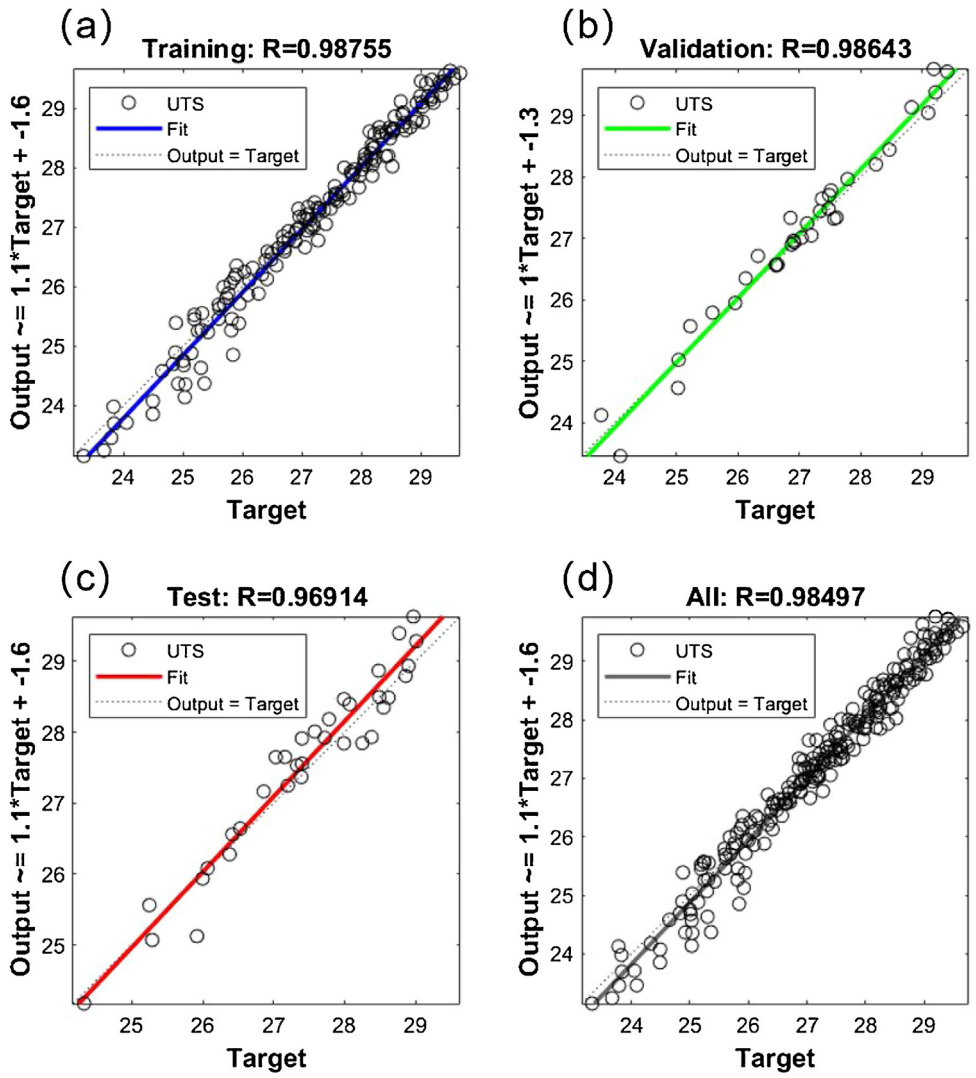

Fig. 4. The predicted ultimate tensile strength values from the machine-learning model as a function of the simulated ultimate tensile strength values for (a) the training set, (b) the validation set, (c) testing data set and (d) all data (The dotted line represents the output data of the model in exactly the same as the target data in the data set; the solid line represents the regression results between the output data and the target data).

validation set gradually increasing, which is over-fitting problem. The existence of over-fitting greatly affects the accuracy of machine learning model, so we need to choose a suitable training epoch to avoid over-fitting. Here, we use cross-validation to tackle the problem. When the MSE of the validation set shows an upward trend with the increase of training epochs, we stop training to obtain the best training epoch, which is also called "early stopping strategy". Fig. 5 indicates correlation between MSE of training set, validation set, testing set, and training epoch.

To further verify the accuracy of the machine-learning model, we should compare the predicted data and the simulated data, which is not in our build database. Here, the predicted and simulated values for $Co_{21}Cr_{20}Ni_{59}$, $Co_{29}Cr_{30}Ni_{41}$, and $Co_{49}Cr_{30}Ni_{21}$ MEA ultimate tensile strengths beside the constructed database are compared in Table 1. These data comes from different compositional regions, which include the minimum strength region, medium strength region, and maximum strength region. In Table 1, the relative errors between the predicted and simulated values are within 2 %, indicating that our machine- learning model can accurately predict the tensile strengths of MEAs. However, why is the machine-learning model so accurate? The current model uses the three independent variables to fit one variable, which is a

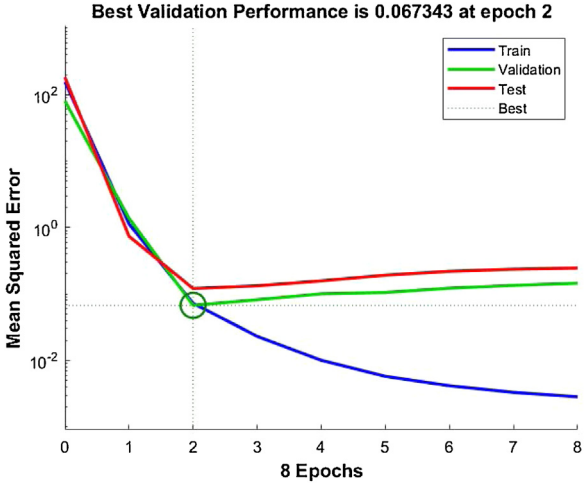

Fig. 5. The mean squared error (MSE) between predicted and simulated values from the "chemical composition - UTS" model as a function for the training set, the validation set and the testing set with the increase of training epochs. It can be seen that the epoch and MSE of the stopping point (the point with best performance) are 2 and 0.067, respectively.

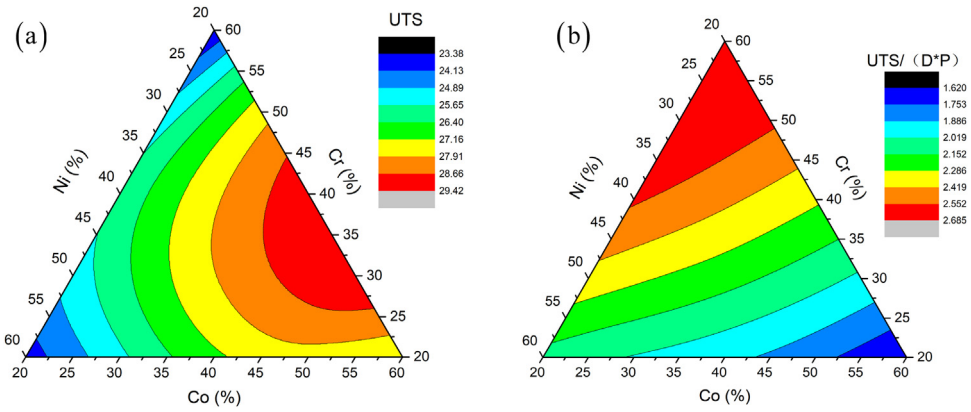

Fig. 6. The distribution of ultimate tensile strength (a) and ultimate tensile strength/(density × price) (b).

Table 1
The strength and error in different compositional regions.

System	MD result (GPa)	Machine learning result (GPa)	Error (%)
Co21Cr20Ni59	23.5	23.9	1.7
Co29Cr30Ni41	26.7	26.9	0.7
Co49Cr30Ni21	29.4	29.2	0.7

Table 2
The density and price of pure element.

Element	Density (g/cm^3)	Price ($/kg)
Co	8.9	3.88
Cr	7.2	0.86
Ni	8.9	1.58

"dimension-reduction fitting", and thus our model is very reliable for predicting the tensile strength.

Now, based on our machine-learning model, we can use this model instead of MD simulations to obtain the ultimate tensile strengths of $Cr_xCo_yNi_{100-x-y}$ MEAs in a wide range of elemental compositions. Here, we predict the ultimate tensile strength of $Cr_xCo_yNi_{100-x-y}$ MEA ($20 \le x \le 60$ at.%, and $20 \le y \le 60$ at.%) with x and y changing in steps of 0.1. That is to say, we have traversed all possible cases of $Cr_xCo_yNi_{100-x-y}$ MEA ($20 \le x \le 60$ at.%, and $20 \le y \le 60$ at.%), and there are 80,601 cases in total. Fig. 6(a) shows the distribution of the ultimate tensile strengths in $Cr_xCo_yNi_{100-x-y}$ MEAs. With the increase of the target values of ultimate tensile strengths, the concentrations of Co and Cr elements become larger. In fact, $Cr_xCo_yNi_{100-x-y}$ MEAs are generally composed of an FCC Ni-based solid solution as the dominant phase, and the second and third phases are a Cr-like BCC solid solution and a Co-like HCP solid solution, respectively [33–35]. We fix the concentration of the Cr element and set it to lower than 50 %. In other words, the total concentration of the Co + Ni elements is higher than 50 %. When the concentration of Co keeps rising, the concentration of the Ni-based FCC-dominant phase continues to decrease. The concentration of the Co-like HCP phase increases, while most of the Cr element exists in the Cr-like BCC phase, which will not change basically. It is well known that the strengths of Co and Cr are greater than that of Ni. Hence, when the Cr concentration is lower than 50 %, the strengths of $Cr_xCo_yNi_{100-x-y}$ concentration of Cr element higher than 50 %. In other words, the Cr-like BCC phase plays a leading role in affecting the ultimate tensile strength. As a result, the increase in the concentration of the Co element leads to slowly increase the ultimate tensile strength (Fig. 6(a)).

However, if we blindly pursue the high strengths of alloys, it may lead to a high cost and high density of the alloy due to the difference of the density and price of each element, thus limiting its large-scale use. Here, the density and price of a pure element are shown in Table 2, to be used to calculate the product of the density and price in $Cr_xCo_yNi_{100-x-y}$ MEAs. To search for the optimumal elemental composition in $Cr_xCo_yNi_{100-x-y}$ MEAs with the high strength and low cost/density, we use a principle "ultimate tensile strength/(density × price)" to describe a combination performance of $Cr_xCo_yNi_{100-x-y}$ MEAs, where "ultimate tensile strength/density" refers to specific strength of the alloys [36] and "specific strength/price" denotes specific strength per unit price. Fig. 6(b) shows the distribution of the ultimate tensile strength/(density × price) in $Cr_xCo_yNi_{100-x-y}$ MEAs. The finding indicates an increasing trend with the decrease of the Cr composition. When the composition of Cr ranges from 50 to 60 at.%, the combination performance of $Cr_xCo_yNi_{100-x-y}$ MEAs is better. In fact, as mentioned above, although the strengthening ability of Cr is not as obvious as Co, Cr has low density and low price advantages. Therefore, when designing a high-strength low-density/price CoCrNi MEA, the proportion of the Cr element should be relatively larger.

To quickly and accurately determine the optimal material composition for advanced materials with target properties, exploring the vast amount of potential compositions cannot be coped with experiments alone and computational methods are therefore crucial [37–39]. To tackle the challenge of established composition-property relationship, we proposed a new approach "high-throughput MD simulation combined machine learning". The main advantages of this approach are that it not only can accurately predict the yield strength of MEA in a wide range of elemental compositions, but also greatly reduces the need of experiment and calculation. In future, using high-throughput experimental technologies combined with the optimized composition range of MEAs from the current work, the advanced MEAs with optimum comprehensive properties would be developed at a low cost and time.

4. Conclusion

High-throughput MD simulation combined machine learning was used to predict the the optimum elemental composition for $Cr_xCo_yNi_{100-x-y}$ MEA with high strength and low cost/density. For predicting the high strength and low cost/density, the performance of the machine learning models was found to be best using ANN. The machine learning models show good performance for the ultimate tensile strength. We believe that the machine learning models developed in this work can be used to accurately predict the unseen data of MEA. The outstanding contribution of our work is to propose the methods of ḧigh throughput simulation combined with

machine learning, which can not only obtain a large number of data quickly and accurately, but also help us to establish the relationship between the composition and mechanical properties of MEAs. Moreover, the composition range of MEAs with the best mechanical properties would give the initial reference value to guide the experiment accurately, comparing with the traditional "trial and error" method. This work indicates great potential of high-throughput MD simulation combined machine learning in the design of advanced materials with target properties.

Declaration of Competing Interest

The authors report no declarations of interest.

Acknowledgements

This work was supported financially by the Foundation for Innovative Research Groups of the National Natural Science Foundation of China (No. 51621004), the National Natural Science Foundation of China (Nos. 51871092, 11772122, 51625404, 51771232, and 51671217), the State Key Laboratory of Advanced Design and Manufacturing for Vehicle Body (No. 71865015), the State Key Laboratory of Powder Metallurgy, and the National Key Research and Development Program of China (Nos. 2016YFB0700300 and 2016YFB1100103). P.K. Liaw very much appreciates the support of the U.S. Army Research Office Project (Nos. W911NF-13-1-0438 and W911NF-19-2-0049) with the program managers, Drs. M.P. Bakas, S.N. Mathaudhu, and D.M. Stepp. P.K. Liaw thanks the support from the National Science Foundation (Nos. DMR-1611180 and 1809640) with the program directors, Drs. J. Yang, J.G. Shiflet, and D. Farkas.

References

[1] B. Gludovatz, A. Hohenwarter, D. Catoor, E.H. Chang, E.P. George, R.O. Ritchie, Science 345 (2014) 1153–1158.
[2] Z.F. Lei, X.J. Liu, Y. Wu, H. Wang, S.H. Jiang, S.D. Wang, X.D. Hui, Y.D. Wu, B. Gault, P. Kontis, D. Raabe, L. Gu, Q.H. Zhang, H.W. Chen, H.T. Wang, J.B. Liu, K. An, Q.S. Zeng, T.G. Nieh, Z.P. Lu, Nature 563 (2018) 546.
[3] T. Yang, Y.L. Zhao, Y. Tong, Z.B. Jiao, J. Wei, J.X. Cai, K. Lu, Y. Liu, C.T. Liu, Science 362 (2018) 933–937.
[4] Z. Li, K.G. Pradeep, Y. Deng, D. Raabe, C.C. Tasan, Nature 534 (2016) 227–230.
[5] Y. Zhang, T.T. Zuo, Z. Tang, M.C. Gao, K.A. Dahmen, P.K. Liaw, Z.P. Lu, Prog. Mater. Sci. 61 (2014) 1–93.
[6] O.N. Senkov, D.B. Miracle, Acta Mater. 122 (2015) 448–511.
[7] P. Shi, W. Ren, T. Zheng, Z. Ren, X. Hou, J. Peng, P.K. Liaw, Nat. Commun. 10 (2019) 489.
[8] C. Lee, G. Song, M.C. Gao, R. Feng, P. Chen, J. Brechtl, Y. Chen, K. An, W. Guo, J.D. Poplawsky, S. Li, A.T. Samaei, W. Chen, A. Hu, H. Choo, P.K. Liaw, Acta Mater. 160 (2018) 158–172.
[9] Y.Z. Shi, L. Collins, N. Balke, P.K. Liaw, B. Yang, Appl. Surf. Sci. 493 (2018) 533–544.
[10] Y.Z. Shi, L. Collins, R. Feng, C. Zhang, N. Balke, P.K. Liaw, B. Yang, Corros. Sci. 133 (2018) 120–131.
[11] Y.Z. Shi, B. Yang, X. Xie, J. Brechtl, K.A. Dahmen, P.K. Liaw, Corros. Sci. 119 (2017) 33–45.
[12] J. Li, H.T. Chen, S. Li, Q. Fang, Y. Liu, L. Liang, H. Wu, P.K. Liaw, Mater. Sci. Eng. A 760 (2019) 359–365.
[13] T.M. Smith, B.D. Esser, N. Antolin, A. Carlsson, R.E.A. Williams, Nat. Commun. 7 (2016) 13434.
[14] M. Calcagnotto, D. Ponge, D. Raabe, Metall. Mater. Trans. A 43 (2012) 37–46.
[15] J. Hu, Y.N. Shi, X. Sauvage, G. Sha, K. Lu, Science 355 (2017) 1292–1296.
[16] M.J. Harvey, G.D. Fabritiis, Drug Discov. Today 17 (2012) 1059–1062.
[17] S. Doerr, M.J. Harvey, F. Noe, G.D. Fabritiis, J. Chem. Theory Comput. 12 (2016) 1845–1852.
[18] I. Buch, M.J. Harvey, T. Giorgino, D.P. Anderson, G.D. Fabritiis, J. Chem. Inf. Model. 550 (2010) 397–403.
[19] G. Hautier, A. Jain, H.L. Chen, C. Moore, S.P. Ong, G. Ceder, J. Mater. Chem. 21 (2011) 17147–17153.
[20] A. Jain, G. Hautier, C.J. Moore, Comput. Mater. Sci. 50 (2011) 2295–2310.
[21] J. Schmidhuber, Neural Netw. 61 (2015) 85–117.
[22] Y. Zhang, S. Yang, J. Evans, Acta Mater. 56 (2008) 1094–1105.
[23] M. Rupp, A. Tkatchenko, K.R. Müller,Phys. Rev. Lett. 108 (2012), 058301.
[24] B. Meredig, C. Wolverton, Nat. Mater. 12 (2013) 123.
[25] L. Ward, A. Agrawal, A. Choudhary, C. Wolverton, NPJ Comput. Mater. 2 (2016) 16028.
[26] Y. Lin, J. Zhang, J. Zhong, Comput. Mater. Sci. 43 (2008) 752–758.
[27] N.S. Reddy, J. Krishnaiah, H.B. Young, J.S. Lee, Comput. Mater. Sci. 101 (2015) 120–126.
[28] M.S. Ozerdem, S. Kolukisa, Mater. Des. 30 (2009) 764–769.
[29] W.M. Choi, Y.H. Jo, S.S. Sohn, S. Lee, B.J. Lee, NPJ Comput. Mater. 8 (2018) 1–9.
[30] V. Nourani, H. Gökçekuş, I.K. Umar,Environ. Res. 180 (2020), 108852.
[31] A.K. Jain, K. Mao, K.M. Mohiuddin, Computer 29 (1996) 31–44.
[32] J. Li, J.H. Cheng, J.Y. Shi, F. Huang, Advances in Computer Science and Information Engineering, Springer, 2012, pp. 553–558.
[33] M. Igor, C. Jan, K. Zuzana, N. Jitka, K. Michael, N. Erich, K. Ivo, H. Vit, D. Ivo, Mater. Sci. Eng. A 701 (2017) 370–380.
[34] B. Wang, H.Y. He, M. Naeem, S. Lan, S. Harjo, T. Kawasaki, Scr. Mater. 155 (2018) 54–57.
[35] L. Wei, Y. Liu, Q. Li, Y.F. Cheng, Corros. Sci. 146 (2019) 44–57.
[36] W. Xu, N. Birbilis, G. Sha, Y. Wang, J.E. Daniels, Y. Xiao, M. Ferry, Nat. Mater. 14 (2015) 1229–1235.
[37] M.C. Troparevsky, J.R. Morris, P.R. Kent, A.R. Lupini, G.M. Stocks,Phys. Rev. X 5 (2015), 011041.
[38] C. Haase, F. Tang, M.B. Wilms, A. Weisheit, B. Hallstedt, Mater. Sci. Eng. A 688 (2017) 180–189.
[39] Y. Lederer, C. Toher, K.S. Vecchio, S. Curtarolo, Acta Mater. 159 (2018) 364–383.